Negative refraction in a photonic crystal with a metallic cross lattice basis

Mark S. Wheeler,* J. Stewart Aitchison, and Mohammad Mojahedi
The Edward S. Rogers Sr. Department of Electrical and Computer Engineering, University of Toronto, 10 King's College Road, Toronto, Ontario, Canada M5S 3G4

(Received 16 August 2004; revised manuscript received 23 November 2004; published 8 April 2005)

A metamaterial with a negative effective index of refraction is made from a two-dimensional square lattice photonic crystal with a metallic cross lattice basis. A simple procedure is given to design a negative index band within a desired frequency range. The operating frequency is made sufficiently low so as to avoid high orders of diffraction from a slab. An effective index of −1, which is a requirement for perfect lensing, is designed. In addition, the structure is optimized to exhibit the largest possible bandwidth of negative refraction, while ensuring an isotropic response and efficient coupling from free space. Simulation results show negative refraction of a Gaussian beam through a prism of such a metamaterial. The simplicity and versatility of the structure make it a suitable candidate for frequencies into the infrared region. The dispersive nature of the metallic crosses and planar fabrication are also discussed.

DOI: 10.1103/PhysRevB.71.155106 PACS number(s): 78.20.Ci, 41.20.Jb, 42.30.−d, 42.70.Qs

I. INTRODUCTION

In the past few years, there has been much interest in the design of metamaterials with a negative index of refraction. Perhaps the most intriguing application of these metamaterials is the perfect lens, which can regenerate the entire wavenumber spectrum of the source at the image plane.[1] This proposition has created much excitement and the development of these metamaterials has been rapidly progressing for the microwave regime,[2,3] with the hope of also demonstrating a negative index of refraction (NIR) at terahertz and infrared frequencies. Photonic crystals (PCs) are structures with periodic arrangements of dielectrics or metals, and are one possible way of synthesizing an effective NIR. This approach has been previously reported and verified numerically,[4–8] with some experimental demonstrations of point imaging by flat slabs at microwave frequencies.[8,9] However, there are a number of outstanding practical issues which should be considered. For example, Notomi's early negative index PC design,[4] which relies on the isotropic behavior of a properly shaped high-order band near the center of the Brillouin zone, operates at frequencies above the Bragg frequency. Consequently, losses may be attributed to higher orders of diffraction.[6,8,10] In addition, the compatibility of the modes of high-order bands with free space in all directions is crucial, yet rarely verified. The more recent use of the anisotropic behavior of a PC near the Brillouin-zone corners[5] can solve some of these issues, but this places a restriction on the lattice orientation if the PC were shaped as a flat slab or a prism and, as implied, the response is no longer isotropic. More importantly, this anisotropic behavior and a collimation effect have been cited as reasons for the imaging effect, rather than negative refraction itself.[11–14] It is clear that there are practical limitations which need to be addressed with either negative-index PC design. The goal of this work is to explore and overcome the limitations of the plane-wave refraction in PC metamaterials that relies on high-order isotropic bands.

This paper presents the use of a metallic cross lattice basis in a two-dimensional photonic crystal (2DPC) in order to synthesize an effective NIR. The cross basis offers a degree of freedom beyond the conventionally studied PCs with a cylindrical rod basis, and consequently provides more versatility and ease of design. A metallic PC is chosen with the intention of decoupling the effects of the basis geometry and the background dielectric constant on the overall shape of the band structure. Furthermore, it is observed that the shape of the band structure for a metallic PC with cross basis is much different from that of a PC with cylindrical rod basis, and as such it facilitates a more "tunable" response. Moreover, the cross basis allows one to design a NIR at frequencies sufficiently low so as to eliminate the large losses due to high orders of diffraction. The low-frequency range also provides the opportunity to design the PC to have an effective index of −1, which is a necessary criterion for "perfect" focusing.[1] An example design with this value of index will be presented. It should be noted that an effective index of −1 has not been possible with other isotropic PC designs.

This paper is organized as follows. Section II reviews the theory of a negative effective index of refraction in PCs. Section III introduces the metallic cross basis and the numerical methods used for calculating band structures. Section IV discusses the band structure of the proposed metamaterial and a design method. Section V shows the time-domain simulation of negative refraction for a Gaussian beam propagating through such a 2DPC. Finally, Sec. VI summarizes the results, and includes the dispersive and lossy nature of metals in the analysis of a 2DPC with cross basis suitable for operation at far-infrared frequencies. A few remarks on the possible fabrication of such a device are also provided.

II. NEGATIVE REFRACTION IN PHOTONIC CRYSTALS

The theory by Notomi[4] described wave propagation in PCs. That work presented a simple method aimed at analyzing plane-wave propagation in periodic structures by using the equifrequency surfaces (EFSs) of the band structure and their gradients. It was shown that an effective index of re-

fraction may be assigned to a 2DPC for frequency ranges in which the EFSs are circular. Thus, for a PC, an isotropic effective index of refraction may be defined and used in the sense of Snell's law. This effective index conveniently encapsulates the response of an otherwise inhomogeneous PC based on the directions of the group velocities. It was also shown that this effective index of refraction could even be negative.[4,6] This is the case if an EFS decreases in radius (wave number) with increasing frequency. Equivalently, this may be recognized in the photonic band structure as a band with downward curvature, or negative second derivative, about the Γ point.

Ideally, an effective index would be sufficient to describe the refraction of a beam through a prism or slab made of a PC. However, improper design could allow high orders of diffraction to emerge from a prism, in addition to the main refracted beam. This is the case if for a given frequency and propagation direction the wave is allowed to "see" the full periodicity of the crystal. The PC then acts like a diffraction grating.

To demonstrate how the higher orders of diffraction arise, the method of analysis for wave propagation in reciprocal space will now be reviewed.[4,6] Assume that a 2DPC with a square lattice, cut in the shape of a flat slab, is sandwiched between two semi-infinite regions of free space. Furthermore, assume that a slab of finite width may be analyzed as though it were infinite in extent. Figure 1 shows the reciprocal space representation of the system, with the EFSs for each region superimposed. Note that the EFS for the PC is repeated by an infinite number of translations of the reciprocal-lattice vectors **G**, although only the first few repetitions are shown. The first Brillouin zone is indicated by a dotted square. For simplicity, every EFS in this example is taken to be a circle. A plane wave with wave vector $\mathbf{k}_i$ is incident on the slab from free space with angle θ_i. The phase-matching condition at the incident interface is indicated by a dashed line. Phase matching at the first interface, along with periodicity in reciprocal space, determines the infinite number of wave vectors that are excited within the PC. These are shown as thin (black) arrows. The figure stresses the fact that the periodic Bloch wave implies an infinite superposition of plane waves with the wave vectors $\mathbf{K}+\mathbf{G}$, where **K** is the Bloch wave vector. The group velocities, shown as thick (red) arrows, are the gradients to the EFSs at the points of the wave-vector solutions and, assuming a 2DPC with an effective NIR, they point inward toward the Γ point. Only the phase-matched wave-vector solutions whose group velocities point away from the first interface are chosen, to ensure that energy propagates away from the source (i.e., a positive group velocity within the 2DPC passband). Also note that the group-velocity vectors shown within the PC are identical, emphasizing the well-defined angle of refraction for the 2DPC. On the other hand, the infinite number of wave vectors excited within the PC results in a large number of phase-matching conditions at the second interface. Now, if the free space EFS is large enough due to a high operating frequency, as shown in Fig. 1, more than one of these phase-matching conditions is satisfied for real propagating wave vectors in free space. Thus, in this example, two plane waves would emerge from the PC.

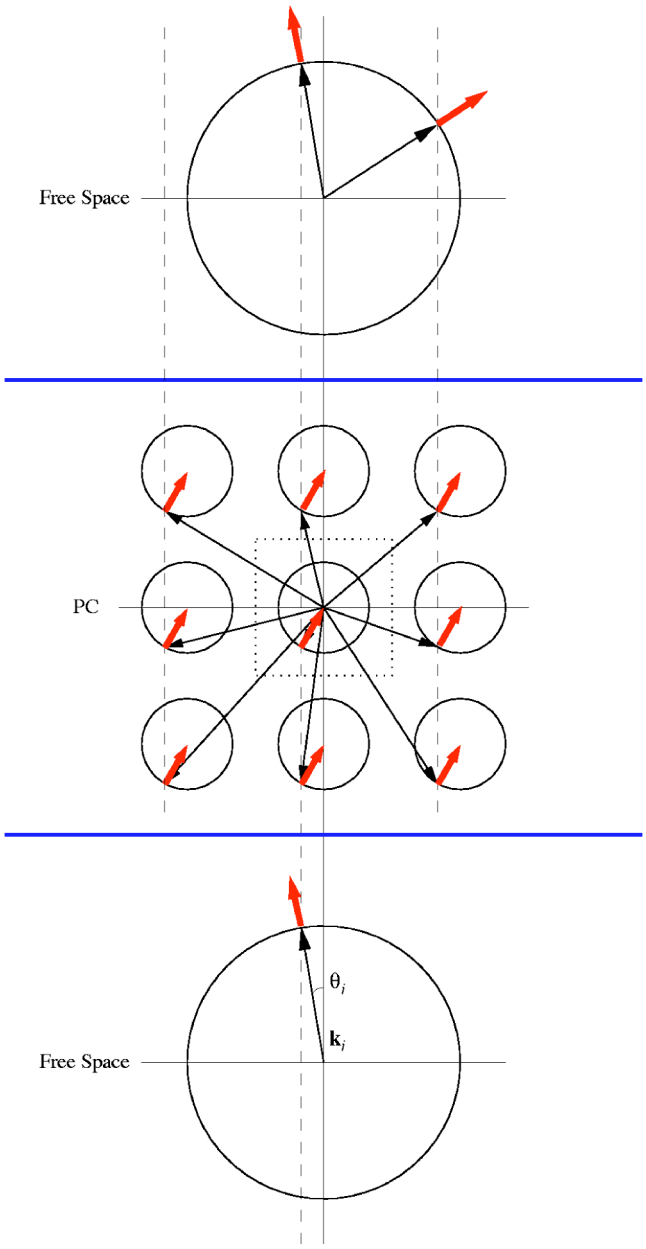

FIG. 1. (Color online) A hypothetical reciprocal space representation of a flat slab of a square lattice PC sandwiched between two semi-infinite regions of free space. The equifrequency surfaces for each medium are shown as circles. Wave vectors are shown as thin black arrows, and group velocities are shown in thick red arrows. The dotted square encloses the first Brillouin zone of the PC, and the vertical dashed lines indicate phase-matching conditions.

The aforementioned high orders of diffraction must be avoided in practical devices. The general example in Fig. 1 was deliberately chosen to illustrate that this diffraction may arise when the size of the free space EFS approaches or exceeds the size of the first Brillouin zone. The problem would be avoided if the NIR could be designed at a frequency such that the size of the free space EFS was sufficiently small. For the case of the square lattice with lattice constant a, this yields a rough bound on the normalized frequency as $\omega a/2\pi c < 0.5$. Since the lattice arrangement and

spacing also play a part in diffraction, a more specific bound would only be appropriate for each specific case.

Moreover, inspection of Fig. 1 shows that the effective index of the 2DPC in this example is within the range $-1 < n_{\text{eff}} < 0$. However, it is easy to see that $n_{\text{eff}} = -1$ requires the EFS of the PC to have the same radius as that of free space. This equality implies that the normalized frequency is limited to $\omega a/2\pi c < 0.5$, which happens to coincide with the previously stated result regarding diffraction.

The origin of high orders of diffraction and the range of effective index values are hence intimately connected with the operating frequency. As has been discussed, low frequencies are more suitable for practical situations. However, it is difficult to design PCs with cylindrical rods which avoid these deficiencies. Moreover, a negative effective index in such 2DPCs is necessarily found in the higher-order bands, which makes it particularly difficult to redesign dielectric PCs at lower frequencies without altering the shape of the band structure and destroying the negative index behavior.

A simple method to avoid high orders of diffraction is to operate within the first band and *necessarily* away from the Γ point. Using a square lattice PC, a negative angle of refraction can be found in the first band about the M point.[5,7] However, this places a restriction on the lattice orientation; the normal to the PC interface must be in the ΓM direction. For a square lattice PC, this implies that only parallel interface slabs are possible; for example, a 45° prism would require one of the normals to be in the ΓX direction. Equally important is the fact that the NIR region is also less isotropic, due to the fashion in which the band structure is rounded at the Brillouin-zone edges. These issues make this design a more challenging candidate for practical devices.[11]

This section has shown that there are a few concerns that must be addressed if PCs are to be considered *practical* media which exhibit an effective NIR. For example, the response of the bands exhibiting a NIR should be easily "tunable" in the design procedure with sufficient isolation from the other bands. The higher orders of diffraction must be eliminated by maintaining a low-frequency range (i.e., $\omega a/2\pi c < 0.5$). The crystal response must be as isotropic as possible (circular EFSs). The EFSs should be centered about the Γ point so that there is no limitation on the lattice orientation. Finally, one should be able to couple efficiently from free space to the desired NIR band.

In the following section a lattice basis is introduced which allows for easier design of bands with a NIR. This basis is used in place of the standard choice of cylindrical rods. A simple design process is given, and solutions to the *practical issues* raised above are provided.

III. METALLIC CROSS BASIS ELEMENT

A PC, which in the strict sense is an infinitely extended periodic structure, is described by a Bravais lattice and a crystal basis. Recent studies of negative refraction in 2DPCs have used lattices with a cylindrical rod basis composed of either dielectric or metal. The reciprocal lattice vectors dictate the plane-wave composition of the Bloch wave function, while the basis geometry and dielectric contrast determine the magnitude of the plane-wave components. This defines how the band structure is distorted from the light cone, and as such will be the starting point in our study of a new basis which can be used to address the practical issues mentioned in Sec. II.

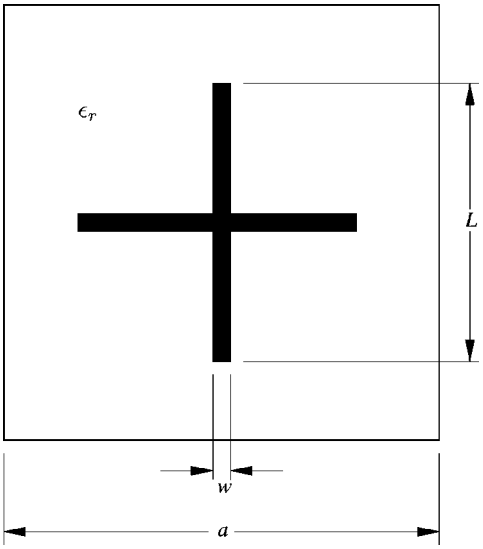

FIG. 2. Schematic of the cross basis. The length of the cross arm is L, the arm width is w, and a is the lattice constant. The remainder of the unit cell is a background dielectric with relative permittivity ϵ_r.

A. Basis geometry

The metallic cross basis is depicted in Fig. 2. The cross arm length is L, each arm width is w, and the length of the square unit cell (the lattice constant) is a. The background dielectric has relative permittivity ϵ_r.

Only a two-dimensional square lattice is considered. Thus the features of the PC are uniform in the third dimension. This implies that the electromagnetic field may be decoupled into two independent polarizations, TE and TM. This work only considers the TE (H-polarized) case, in which the single magnetic-field component is perpendicular to the plane of periodicity, and the electric field is confined to the plane.

Metal has been chosen for the cross basis to exploit an important property. A perfect metal may be considered as having a dielectric constant with an infinite real part. For a given basis geometry, the extreme dielectric contrast between the metallic basis and the background dielectric provides a maximum amount of band distortion from that of free space, which in turn aids in designing well-isolated negative index bands. The use of metal also frees one to design the band structure with a preferred geometry (e.g., crosses in free space), and then *scale the frequency response by replacing the background dielectric without altering the shape of the band structure*. That is, whether the background is air, other dielectric, or semiconductor, the dielectric contrast ratio between the metallic basis and the background remains practically unchanged. However, a possible downside in using a metallic basis, especially for optical frequencies, is the lossy

and dispersive nature of metals; this will be considered in Sec. VI.

A PC with a metallic cross basis has another advantage over the commonly studied cylindrical basis in that the band structure for the former is quite different from the latter. In essence, the magnitudes by which neighboring scatterers interact with each other are given by the basis geometry; in the case of metallic crosses this results in a qualitatively different dispersion diagram $(\omega, \mathbf{K})$ with more bands that are spectrally isolated. Although in general many bands may have the curvature which indicates a negative effective index, they are most often "contaminated" by the presence of other bands in the same frequency range. Thus the increased isolation provided by the cross basis in turn results in potentially more bands with an isotropic negative effective index.

B. Band-structure calculation methods

A number of methods are available for calculating a 2DPC band structure, with the plane-wave expansion[15] being the most popular. However, the metallic cross basis and fine spatial features are not suitable for use with this method. In principle, a perfect metal could be approximated by a dielectric with an infinite real part. The calculations could be improved by using a Drude model, which in turn would require the diagonalization of an enlarged matrix,[16] consequently increasing the memory requirements and computation time. Finally, the fine spatial features of the cross basis implies a Fourier series in reciprocal space which decays slowly; a large and potentially prohibitive number of plane waves would be required in the expansion. Hence, the plane-wave expansion method is not suitable for calculating the band structure of our 2DPC.

The finite difference time-domain (FDTD) method[17] was used to compute all band structures considered in this work. A unit cell of the square lattice PC was discretized into a 50×50 grid. A value of relative permittivity was assigned to every cell. The regions of perfect metal were defined by setting all components of the electric field within and tangential to the metal equal to zero. A broadband source was applied by exciting the magnetic field at a point in the unit cell with a temporal Gaussian profile. Periodic boundary conditions were applied, with opposite pairs of boundaries related by their respective components of a chosen Bloch wave vector **K**.

The band structure was calculated by running many simulations, each defined by a different Bloch wave vector. For each Bloch wave vector, the spectrum of the simulated steady-state time series would give the mode eigenfrequencies. Usually, the fast Fourier transform (FFT) would be used to find this spectrum. However, a long time series would be needed to accurately calculate the eigenfrequencies and provide the fine spectral resolution to resolve closely spaced modes. When calculating an EFS with many wave vectors, the overall simulation time could be extremely long.

The eigenfrequencies can also be found from a much shorter time series. The matrix pencil (MP) method[18–20] can perform a total least-squares estimate of the frequencies of a short time series. For brevity, we refer the interested reader to a short review of the MP method in Ref. 20. The simulation need only be as long as a few cycles of the lowest anticipated frequency. A combination of short FDTD simulations and MP method was used here to calculate full band structures and EFSs in only a few minutes, as compared to hours.

IV. DESIGN PROCEDURE

The design procedure for this metallic PC is fairly simple. The infinite dielectric contrast of the perfect metal allows one to engineer the band structure with only the basis geometry. That is, the shape of the band structure is independent of the background dielectric. After the design of the band-structure shape has been finished, a background dielectric is chosen to scale the designed negative index band to the desired lower operating frequency range, without disrupting the chosen band shape. This scaling procedure is crucial in avoiding high orders of diffraction and achieving $n_{\text{eff}} = -1$.

A. Band engineering

The first stage in designing a NIR band is to create the desired downward band curvature, regardless of the frequency range or band number. This step involves choosing the two free parameters in the cross geometry, L and w. For very small values of both parameters, the band structure is only slightly perturbed from a folded light cone. As the values of these parameters are increased, the bands may change curvature, flatten out, and shift in frequency. This occurs in any 2DPC, yet the band structure of a metallic cross basis and a rod basis change in quite different ways. For narrow crosses (small w), there exists a significant range of values of the cross length L that results in one or even two high-order bands with the correct curvature and isolation, and thus an effective NIR.

It is difficult to give a full quantitative description for this increased isolation in the band structure. However, concepts from the plane-wave expansion method[15] can be used to illustrate how the basis geometry affects the band structure. In particular, the method requires the Fourier series of the reciprocal of the dielectric function. If one were to consider a simple model of a perfect metal as a dielectric with its real part of the permittivity approaching infinity, the components of this series for the crosses would be

$$\epsilon^{-1}(\mathbf{G}) = \frac{1}{\epsilon_r}\left\{ \delta_{\mathbf{G},0} - \frac{Lw}{a^2}\text{sinc}(G_x L/2)\text{sinc}(G_y w/2) - \frac{Lw}{a^2}\text{sinc}(G_x w/2)\text{sinc}(G_y L/2) + \frac{w^2}{a^2}\text{sinc}(G_x w/2)\text{sinc}(G_y w/2)\right\},$$

where ϵ_r is the relative permittivity of the background dielectric, $\mathbf{G} = (G_x, G_y)$ are the reciprocal-lattice vectors, and $\text{sinc}(x) = \sin(x)/x$ with $\text{sinc}(0) = 1$. For the narrow crosses $(w \ll L)$ considered in this work, this function is most appreciable on the G_x, G_y axes, and the rate of decay along each

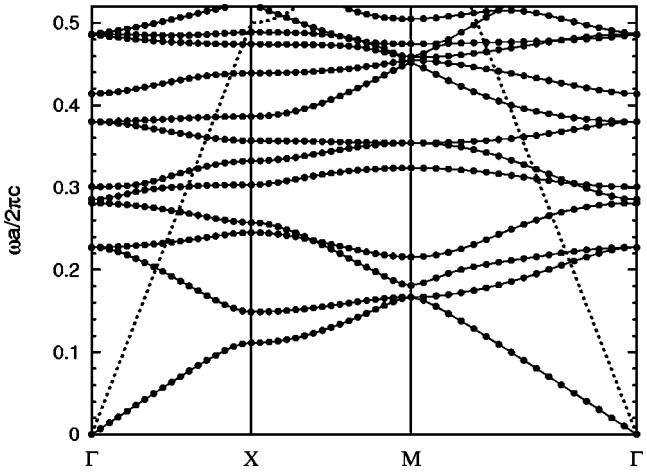

FIG. 3. Band structure of a square lattice 2DPC with perfect metallic crosses of dimensions $L=0.52a$, $w=0.04a$. The field is H polarized and the background dielectric is $\epsilon_r=12$. The bottom edge of the folded light cone is shown in dashed lines.

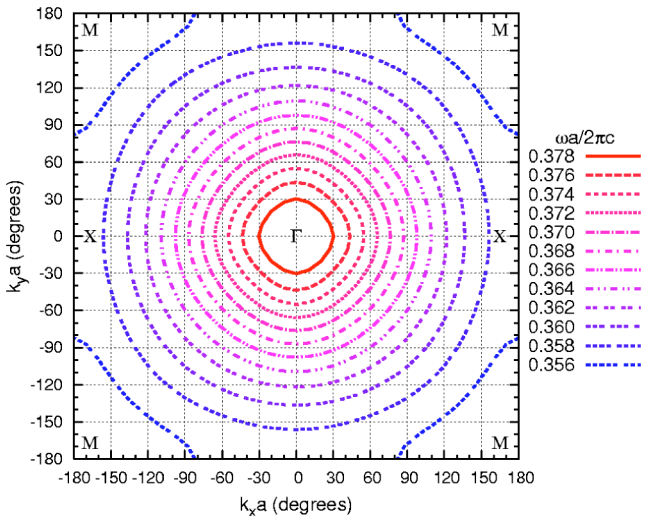

FIG. 4. (Color online) Equifrequency surfaces for frequencies within the seventh band of the dispersion relation ($0.354 \leqslant \omega a/2\pi c \leqslant 0.380$) depicted in Fig. 3.

axis is much less than that due to the Fourier series components of a cylindrical rod.[15] It seems that there is much more complex scattering with the cross basis, and thus a very different and incidentally isolated band structure.

After designing the band-structure shape, the frequency range of the chosen negative index band can be scaled to the desired range below $\omega a/2\pi c<0.5$. If f_0 is the center frequency of the negative index band, and f_0' is the desired center frequency, then the dielectric background ϵ_r may be chosen from the relation $f_0'=f_0/\sqrt{\epsilon_r}$. Adding the dielectric in this way will help avoid the high orders of diffraction for a device manufactured from this PC.

The efficient combination of FDTD and the MP method was used to calculate the band structures for many cross geometries. An example which demonstrates the proper band curvature and isolation is shown in Fig. 3. The cross dimensions are $L=0.52a$, $w=0.04a$, and the background dielectric is $\epsilon_r=12$ (e.g., Si at infrared frequencies). The bottom edge of the free space light cone is also indicated in the figure by dashed lines. The background dielectric was chosen to ensure that the seventh band is scaled to a frequency lower than the first folding of the light cone. This example demonstrates that two high-order bands with a downward curvature about the Γ point are spectrally isolated, i.e., only one band resides in the spectral range it occupies. The fourth band ($0.258 \leqslant \omega a/2\pi c \leqslant 0.281$) and seventh band ($0.354 \leqslant \omega a/2\pi c \leqslant 0.380$) seem to be candidates which have a region of negative effective index of refraction. However, the modes of the fourth band are incompatible with those of free space. This will be discussed later in this section, and so, for the time being, the fourth band will be ignored.

The EFSs for the seventh band are shown in Fig. 4. The gradient for any Bloch wave vector points inward toward the Γ point for all frequencies with circular contours. The circles indicate an isotropic response, and therefore allow for the definition of an effective index in the sense of Snell's law. It is interesting to note that the contours are very close to circles for most of their frequency range. This is mainly because a large amount of band folding has occurred due to the initial high frequency of the band (without the dielectric background) which has resulted in a very circular irreducible zone representation. It is interesting to note that here such a circular EFS was obtained without requiring the use of a triangular lattice. As stated earlier, and as is evident from Fig. 4, scaling down in frequency by introducing the background dielectric has not affected the results adversely.

The band structures for the TM polarization were also calculated. However, the results were similar to the band structures of PCs with a metallic cylindrical basis.[16] That is, the most interesting feature is a band gap from zero frequency to the first band, which is expected for PCs with the electric field polarized in the direction of the continuous metal basis. Unfortunately, the combination of negative index band curvature and band isolation was not present to the same degree as with the TE modes for any of the cross geometries considered. There seems to be no significant advantage in using the TM modes of the metal cross basis PC for the purposes of negative refraction.

B. Range of effective index values

The effective index for the example design of $L=0.52a$, $w=0.04a$, and $\epsilon_r=12$ is shown in Fig. 5. The effective index of refraction is shown as a function of frequency for both the ΓX and ΓM directions. For each direction, the effective index was calculated by using the $(\omega,\mathbf{K})$ pairs from the band structure. In this approach, the effective index is the ratio of the magnitude of the Bloch wave vector to the wave number of free space at the same frequency.[6] The medium is isotropic in the frequency range over which the effective indices in the two principal directions are approximately the same. This will be quantified later in this section. Also note that Fig. 5 shows that this design has $n_{\text{eff}}=-1$ at $\omega a/2\pi c=0.361$.

C. Negative index bandwidth

Although a particular design of a negative index band was shown above, the ease with which the band structure may be designed will now be discussed.

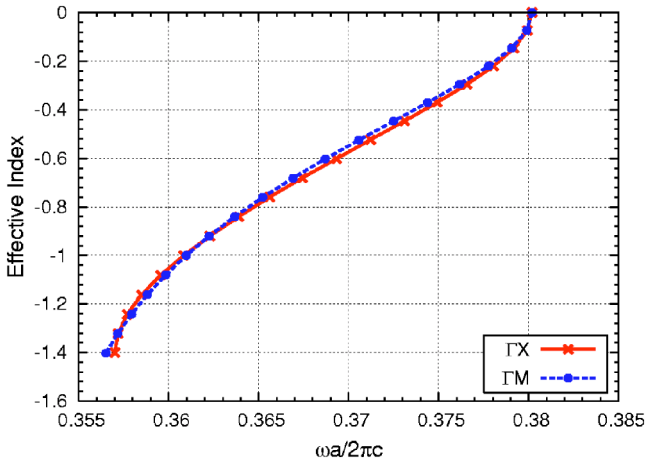

FIG. 5. (Color online) The calculated effective index of refraction as a function of normalized frequency.

The calculated effective indices along the two principal directions ΓX and ΓM were discussed earlier. The index is considered to be isotropic if the normalized difference of the indices in the two principal directions is less than 0.5%. That is, $2|n_{\Gamma X}-n_{\Gamma M}|/(n_{\Gamma X}+n_{\Gamma M})<0.005$. If ω_h is the highest frequency and ω_l is the lowest frequency which satisfy this relation, then the definition of the effective index bandwidth (BW) is taken as $\mathrm{BW}=2(\omega_h-\omega_l)/(\omega_h+\omega_l)$.

The bandwidth of the seventh band as a function of the cross length L for various widths w is shown in Fig. 6. One may design for a given bandwidth by simply consulting a graph such as Fig. 6 in order to choose the appropriate cross dimensions. The designer need not worry about the geometry's effect on the final operating frequency range.

Figure 6 shows that the greatest bandwidth is found for the thinnest crosses. For a given cross with narrow width w, the qualitative progression due to changing the cross length L is as follows. A small length cross has a band structure similar to a slightly perturbed folded light cone, and as such has no spectrally isolated negative index bands. As the length of the cross is increased, the bands flatten out and eventually some become isolated in some spectral regions. This effect seems to be due to the cross geometry, as the same degree of isolation of the bands is not as easily found for a rod basis. When L reaches a threshold value, the seventh band becomes isolated in frequency and is very circular around the Γ point, giving rise to the isotropic bandwidths shown in Fig. 6. As L is further increased, the bandwidth increases to a maximum, and then the band tends to flatten out, and the bandwidth of isotropic response decreases. For sufficiently large L, the eighth band moves downward in frequency into the same spectral range as the seventh band, and causes a sharp decrease in the bandwidth. This is indicated by the steep slopes for large L.

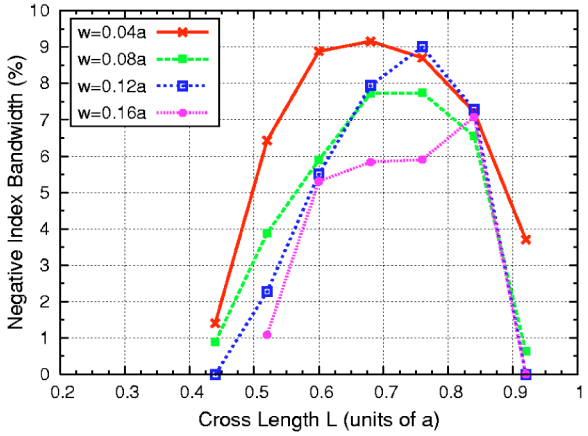

FIG. 6. (Color online) Isotropic bandwidth of the negative index (seventh) band as a function of the overall cross length L. Several cases of cross width w are shown.

D. Mode compatibility with free space and coupling to the PC

So far, our approach has been to use the capabilities of the perfect metal cross basis to easily generate regions of negative effective index. We then utilized the background dielectric to scale down the frequency response, hence making the use of higher-order bands more practical. There is one remaining consequence of using higher-order bands that must now be examined. As stated earlier and shown in Fig. 3, both the fourth band $(0.258\leqslant\omega a/2\pi c\leqslant 0.281)$ and the seventh band $(0.354\leqslant\omega a/2\pi c\leqslant 0.380)$ have the correct curvature and isotropic response for our purposes. However, the mode pattern of the fourth band along the ΓX direction is *not* suitable for coupling from free space. This is not apparent from the information presented in the dispersion relation; the mode patterns must be examined, and are shown in Figs. 7(a)–7(d). The pattern in Fig. 7(a) has odd symmetry about the $y=0$ axis, whereas plane waves have even symmetry about the axis defined by their propagation wave vector. Thus, free space plane waves cannot couple to the modes of the fourth band along the ΓX direction.[21,22] Hence the fourth band, despite its isotropic response and downward curvature, cannot be assigned an effective NIR. On the other hand, there is no such problem with the seventh band, as indicated by Figs. 7(c) and 7(d).

V. PRISM REFRACTION SIMULATION RESULTS

The negative effective index was verified with the refraction of a Gaussian beam through a 2DPC. The values $L=0.52a$, $w=0.04a$, and $\epsilon_r=12$ were again used for our 2DPC with metallic cross basis which was shaped into a prism having $n_{\mathrm{eff}}=-1$. The 45° prism was simulated with the FDTD method,[17] as shown in Fig. 8. Perfectly matched layers were used to truncate the computational domain. Note that the right-hand edge of the prism is matched and truncated by the absorber, so that retroreflections do not obscure the refracted wave; this allows the refracted beam to have sufficient time to settle into a steady-state condition.[23] A source plane parallel to the bottom edge of the figure was excited with a Gaussian spatial profile of sufficient width such that there was little spread in the wave-vector components. This profile was modulated with a sinusoid of frequency $\omega a/2\pi c=0.361$. The beam was normally incident on the lower horizontal face of the prism, along the ΓX direction. The wave

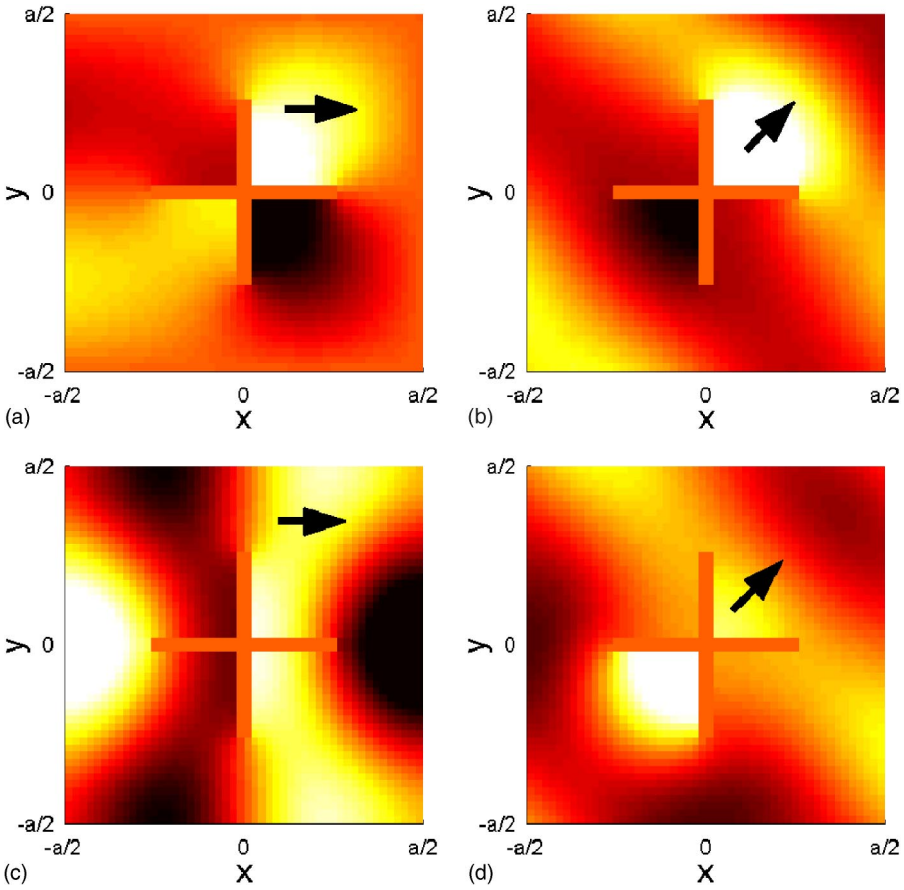

FIG. 7. (Color online) Mode patterns of (a) the fourth band with $k_x a = 101°$, $k_y a = 0°$, $\omega a/2\pi c = 0.270$; (b) the fourth band with $k_x a = 60°$, $k_y a = 60°$, $\omega a/2\pi c = 0.270$; (c) the seventh band with $k_x a = 130°$, $k_y a = 0°$, $\omega a/2\pi c = 0.361$; (d) the seventh band with $k_x a = 92°$, $k_y a = 92°$, $\omega a/2\pi c = 0.361$. The magnitude of the magnetic field is shown. A black arrow in each unit cell indicates the direction of the Bloch wave vector.

propagated through the PC, and was then incident at 45° on the angled face. The negative refraction at this interface is easily seen in the figure, and, more importantly, it is also clear that no higher orders of diffraction are present. This device would not have been possible if it was manufactured from a PC with band structure depicted in Ref. 5 with a downward curvature about the *M* point, since in that case the normal to the interface would have been along the ΓX direction and as such no Bloch mode solution exists.

VI. SUMMARY

A 2DPC with a metallic cross basis was studied in order to design a structure with an effective NIR. A combination of the FDTD and MP methods was used to efficiently investigate the required geometry of the metallic crosses which produced an isotropic and wide bandwidth NIR behavior. The design has the benefits of using a simple square lattice and small filling fraction of metal, a large range of effective NIR values (including −1), low operating frequency, and correct coupling to free space modes. This metallic cross PC allows for flexible design of practical devices, and the important issue of avoiding high orders of diffraction is easily resolved. The structure is simple enough that it should be possible to fabricate at the infrared frequency range. However, the effects of metallic losses and dispersion must then also be included in our analysis, where so far we have only assumed perfect conductors.

The band structures for our 2DPC with metallic cross basis, where the metal now has the Drude dispersion[24]

$$\epsilon(\omega) = 1 - \frac{\omega_p^2}{\omega(\omega - i\gamma)},$$

were also studied. It was found that the frequency dependence of the Drude model only slightly changed the band structure when micron-scale wavelengths were considered. As an example, when we used values typical of gold (i.e., $\omega_p = 9$ eV and $\gamma = 0.01\omega_p$), the NIR range was $0.3558 \leqslant \omega a/2\pi c \leqslant 0.3785$, and the value $n_{\text{eff}} = -1$ occurred at $\omega a/2\pi c = 0.360$. These results are quite similar to those presented in Sec. IV which only considered perfect metals. For the same normalized cross dimensions, a device with $n_{\text{eff}} = -1$ can be constructed at $\lambda = 10.6$ μm (CO_2 laser line) with $a = 3.82$ μm, $L = 1.99$ μm, and $w = 153$ nm. The damping constant γ does not seem to dramatically affect the band structure, although it would define an effective path length within the PC device. This path loss is somewhat minimized due to the small filling fraction of the metal.

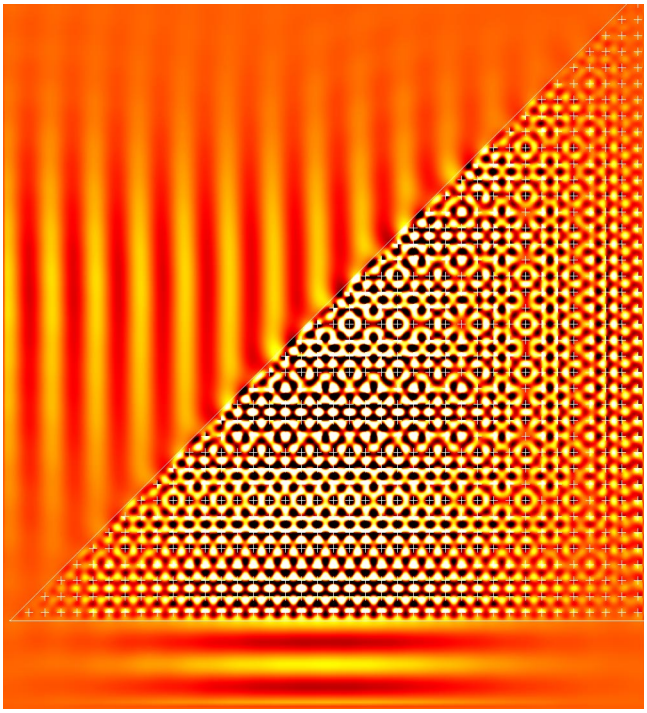

FIG. 8. (Color online) FDTD simulation of negative refraction in a prism made of 2DPC with metallic cross basis. A Gaussian beam was normally incident on the bottom face of the prism. The beam exits the prism with a negative angle of refraction and out to the left edge of the figure.

Two different methods may be used to fabricate a 2DPC metamaterial with these dimensions. The first method would be to etch the cross features into a slab of dielectric or semiconductor substrate (such as Si), and then fill the voids with the metal. The features would have to be deep enough so that the cross section of a beam would be scattered by columns with effectively uniform features in the third dimension. However, the etching of deep, narrow features may be difficult, so a simpler method may be a monolithic planar processing approach. The metamaterial could be built up in a periodic fashion by planar deposition of the metallic cross layers, separated by a thin dielectric or semiconductor spacing layers. To verify the validity of the latter approach, band structures were calculated for three-dimensional unit cells composed of thin metal crosses suspended in a dielectric of $\epsilon_r = 12$. The heights of the cells were increased up to $a/6$, and the phase differences between the cell faces in the third dimension were held at zero. The band structures were essentially unchanged from the results presented earlier for the 2DPC in Fig. 3. The periodicity in the third dimension was kept small enough so that the structure was effectively uniform.

A flat lens is an important device that can be made with negative index metamaterials. The wide range of indices available with the metallic cross basis makes this structure attractive. In particular, the example given in this paper had $n_{\text{eff}} = -1$, which is one of the requirements for a perfect lens,[1] and such a value has not been possible with other PC designs. However, the sub-wavelength resolution of a perfect lens requires careful regeneration of the evanescent components of the source, and further investigation into this regeneration with the metal cross PC is required.

ACKNOWLEDGMENTS

This work was supported by the Natural Sciences and Engineering Research Council of Canada under Grant No. 249531-02, and in part by Photonic Research Ontario, Funded Research No. 72022792.

*Email address: mark.wheeler@utoronto.ca

[1] J. B. Pendry, Phys. Rev. Lett. **85**, 3966 (2000).
[2] D. R. Smith, W. J. Padilla, D. C. Vier, S. C. Nemat-Nasser, and S. Schultz, Phys. Rev. Lett. **84**, 4184 (2000).
[3] G. V. Eleftheriades, A. K. Iyer, and P. C. Kremer, IEEE Trans. Microwave Theory Tech. **50**, 2702 (2002).
[4] M. Notomi, Phys. Rev. B **62**, 10 696 (2000).
[5] C. Luo, S. G. Johnson, J. D. Joannopoulos, and J. B. Pendry, Phys. Rev. B **65**, 201104(R) (2002).
[6] S. Foteinopoulou and C. M. Soukoulis, Phys. Rev. B **67**, 235107 (2003).
[7] C. Luo, S. G. Johnson, J. D. Joannopoulos, and J. B. Pendry, Opt. Express **11**, 746 (2003).
[8] P. V. Parimi, W. T. Lu, P. Vodo, J. Sokoloff, J. S. Derov, and S. Sridhar, Phys. Rev. Lett. **92**, 127401 (2004).
[9] E. Cubukcu, K. Aydin, E. Ozbay, S. Foteinopoulou, and C. M. Soukoulis, Phys. Rev. Lett. **91**, 207401 (2003).
[10] M. Qiu, L. Thylen, M. Swillo, and B. Jaskorzynska, IEEE J. Sel. Top. Quantum Electron. **9**, 106 (2003).
[11] Z.-Y. Li and L.-L. Lin, Phys. Rev. B **68**, 245110 (2003).
[12] L.-S. Chen, C.-H. Kuo, and Z. Ye, Phys. Rev. E **69**, 066612 (2004).
[13] C.-H. Kuo and Z. Ye, Phys. Rev. E **70**, 026608 (2004).
[14] D. N. Chigrin, S. Enoch, C. M. S. Torres, and G. Tayeb, Opt. Express **11**, 1203 (2003).
[15] K. Sakoda, *Optical Properties of Photonic Crystals* (Springer, Berlin, 2001).
[16] V. Kuzmiak and A. A. Maradudin, Phys. Rev. B **55**, 7427 (1997).
[17] A. Taflove and S. C. Hagness, *Computational Electrodynamics: The Finite-Difference Time-Domain Method*, 2nd ed. (Artech House, Norwood, MA, 2000).
[18] Y. Hua and T. K. Sarkar, IEEE Trans. Acoust., Speech, Signal Process. **38**, 814 (1990).
[19] R. S. Adve, T. K. Sarkar, O. M. C. Pereira-Filho, and S. M. Rao, IEEE Trans. Antennas Propag. **45**, 147 (1997).
[20] T. K. Sarkar and O. Pereira, IEEE Antennas Propag. Mag. **37**, 48 (1995).
[21] W. M. Robertson, G. Arjavalingam, R. D. Meade, K. D. Brommer, A. M. Rappe, and J. D. Joannopoulos, Phys. Rev. Lett. **68**, 2023 (1992).
[22] K. Sakoda, Phys. Rev. B **52**, 7982 (1995).
[23] S. Foteinopoulou, E. N. Economou, and C. M. Soukoulis, Phys. Rev. Lett. **90**, 107402 (2003).
[24] R. J. Luebbers, F. Hunsberger, and K. S. Kunz, IEEE Trans. Antennas Propag. **39**, 29 (1991).